JCTC Journal of Chemical Theory and Computation

Article

pubs.acs.org/JCTC

Modeling the Self-Assembly and Stability of DHPC Micelles Using Atomic Resolution and Coarse Grained MD Simulations

Johan F. Kraft,[†] Mikkel Vestergaard,[†] Birgit Schiøtt,*[,†] and Lea Thøgersen*[,‡]

[†]Center for Insoluble Protein Structures (*in*SPIN), Interdisciplinary Nanoscience Center (*i*NANO), Department of Chemistry, Aarhus University, Langelandsgade 140, DK-8000 Aarhus C, Denmark

[‡]Centre for Membrane Pumps in Cells and Disease (PUMPKIN), Bioinformatics Research Centre, C.F. Møllers Alle 8, DK-8000 Aarhus C, Denmark

Supporting Information

ABSTRACT: Membrane mimics such as micelles and bicelles are widely used in experiments involving membrane proteins. With the aim of being able to carry out molecular dynamics simulations in environments comparable to experimental conditions, we set out to test the ability of both coarse grained and atomistic resolution force fields to model the experimentally observed behavior of the lipid 1,2-dihexanoyl-*sn*-glycero-3-phosphocholine (DHPC), which is a widely used lipid for biophysical characterization of membrane proteins. It becomes clear from our results that a satisfactory modeling of DHPC aggregates in solution poses different demands to the force field than do the modeling of bilayers. First, the representation of the short tailed lipid DHPC in the coarse grained force field MARTINI is assessed with the intend of successfully self-assemble micelles with structural characteristics comparable to experimental data. Then, the use of the recently presented polarizable water model in MARTINI is shown to be essential for producing micelles that are structurally in accordance with experiments. For the atomistic representations of DHPC micelles in solution the GROMOS96 force field with lipid parameters by A. Kukol fails to maintain stable micelles, whereas the most recent CHARMM36 lipid parameters and GROMOS96 with the so-called Berger lipid parameters both succeed in this regard.

INTRODUCTION

Membrane bound proteins are important in nature, guiding the exchange of molecules and ions between cells and the environment. However, membrane proteins are difficult to study in their native lipid environment, and therefore several membrane mimics have been used in biophysical characterization of these proteins. The membrane mimics can consist of several different types of detergent or lipid molecules arranged in different assemblies such as micelles, bicelles, and vesicles.[1−5] Membrane proteins embedded in membrane mimics have their membrane spanning part inserted into the hydrophobic part of the mimic. This effectively solubilizes the protein and allows for an easier handling of the protein of interest.

Before studying the properties of membrane proteins inserted in membrane mimics, it is important to understand the behavior of the lipid membrane mimic in question to envision how it may affect the protein. By using molecular dynamics (MD) simulations it is possible to model membrane proteins inserted in either a membrane mimic as used experimentally or in a nativelike membrane setting, hereby allowing for comparative studies of the structural and functional effects that the change of membrane environment may have on the protein.[6] While atomic resolution simulations are well established, the use of a more coarse grained representation of lipids, water, and protein allows for the description of dynamics on the microsecond time scale and the study of systems involving thousands of molecules. Using a coarse grain (CG) force field it is thus possible to follow the self-assembly of a membrane mimic leading to the formation of aggregates and the equilibration of these. Naturally, such studies rely on a proper CG description of the lipid or detergent molecule in water. The high time- and spatial resolution resulting from atomistic MD simulations is still of great interest, as this will often hold information on detailed molecular interactions not readily accessible by any other methods, neither experimental nor theoretical. In particular it is a great advantage if a CG model is chosen where the mapping to atomistic resolution (reverse CG) is defined, such that MD simulations can be carried out with access to both the microsecond time scale and the detailed atomistic interactions. To carry out reliable simulations in both the atomic resolution and CG representations, one must ensure that the model description of the lipids and detergent molecules involved in the membrane mimic results in simulation behavior consistent with experimental knowledge.

In the study presented here, the focus is on micelles made out of DHPC lipids. Micelles are close to spherical aggregates of detergent-like molecules, which can cover the hydrophobic surface of a membrane protein[1] to make it effectively water-soluble. DHPC is often used in micelles as well as in bicelles, which are disklike membrane mimics formed by mixtures of long- and short lipid molecules,[4] especially in relation to liquid state NMR studies.[7,8] In this study we inspect different CG representations of a setup consisting of DHPC lipids and water modeled with the MARTINI CG force field.[9] We examine the self-assembly and various physicochemical properties of DHPC micelles in microsecond MD simulations where the salt

Received: December 22, 2011
Published: March 10, 2012

Table 1. Overview of the 16 Simulations Carried out in This Study[a,b]

simulation name	water model	lipid model	starting structure	#ions	[NaCl] (mM)	T (K)	#lipids	time
NaCl150T298PWst	polarizable	MARTINI 1 tail bead	random	750 Na^+ 750 Cl^-	150	298	1000	2 μs
NaCl150T298Wst	**standard**	MARTINI 1 tail bead	random	750 Na^+ 750 Cl^-	150	298	1000	2 μs
NaCl0T298PWst	polarizable	MARTINI 1 tail bead	random	**0 Na^+ 0 Cl^-**	**0**	298	1000	2 μs
NaCl0T298PWlt	polarizable	**MARTINI 2 tail beads**	random	**0 Na^+ 0 Cl^-**	**0**	298	1000	2 μs
NaCl0T298Wlt	**standard**	**MARTINI 2 tail beads**	random	**0 Na^+ 0 Cl^-**	**0**	298	1000	2 μs
NaCl0T298Wst	**standard**	MARTINI 1 tail bead	random	**0 Na^+ 0 Cl^-**	**0**	298	1000	2 μs
W-NaCl150T298PWst	**standard**	MARTINI 1 tail bead	**NaCl150T298PWst after 2 μs**	750 Na^+ 750 Cl^-	150	298	1000	2 μs
PW-NaCl150T298Wst	polarizable	MARTINI 1 tail bead	**NaCl150T298Wst after 2 μs**	750 Na^+ 750 Cl^-	150	298	1000	2 μs
NaCl500T298PWst	polarizable	MARTINI 1 tail bead	random	**2500 Na^+ 2500 Cl^-**	**500**	298	1000	2 μs
NaCl1000T298PWst	polarizable	MARTINI 1 tail bead	random	**5000 Na^+ 5000 Cl^-**	**1000**	298	1000	2 μs
NaCl150T285PWst	polarizable	MARTINI 1 tail bead	random	750 Na^+ 750 Cl^-	150	**285**	1000	2 μs
NaCl150T310PWst	polarizable	MARTINI 1 tail bead	random	750 Na^+ 750 Cl^-	150	**310**	1000	2 μs
NaCl150T323PWst	polarizable	MARTINI 1 tail bead	random	750 Na^+ 750 Cl^-	150	**323**	1000	2 μs
NaCl150T298CHARMM	**TIP3P**	**CHARMM36**	**selected aggregates from NaCl150T298PWst**	**175 Na^+ 175 Cl^-**	150	298	**233**	**100 ns**
NaCl150T298Kukol	**SPC**	**GROMOS96 53a6 Kukol lipids**	**selected aggregates from NaCl150T298PWst**	**175 Na^+ 175 Cl^-**	150	298	**233**	**100 ns**
NaCl150T298Berger	**SPC**	**GROMOS96 53a6 Berger lipids**	**selected aggregates from NaCl150T298PWst**	**175 Na^+ 175 Cl^-**	150	298	**233**	**100 ns**

[a]In all simulations the DHPC concentration is 200 mM. [b]The difference between the respective simulation and the simulation in the top row (NaCl150T298PWst) is marked in bold.

concentration and temperature are varied, and we compare the results to available experimental observations. Furthermore, selected DHPC micelles formed in the CG MD simulations are reverse coarse grained (rvCG) to atomistic resolution and simulated for 100 ns to assess the stability of the micelles in three different atomistic force fields. It is expected that atomistic simulations should reproduce experimental observations to a higher degree than seen for CG simulations. However, the simulations presented here illustrate that the complex behavior of detergent-like lipids forming liquid aggregates is challenging also for atomistic resolution force fields. Especially, the assumed transferability of force field parameters applied when parametrizing lipid molecules where only the tail-lengths differ[10−13] seems not to be generally applicable.

METHODS

First, different MARTINI CG representations of both the DHPC lipids and water molecules are inspected. Then it is further examined if the CG model can account for effects induced by changes in temperature or NaCl concentration. Since CG force fields have less detailed properties compared to all atom (AA) simulations, we finally rvCG selected micelles formed during a CG simulation and carry out MD simulations on these using AA and united atom (UA) force fields to investigate the stability of the formed micelles and compare the results to both CG micelles and experiments. An overview of the simulations carried out in this study is provided in Table 1. All simulations have been carried out at a lipid concentration of 200 mM, well above the critical micelle concentration (CMC) of DHPC (11−16 mM).[14−23] The simulations are named throughout the paper by using the following conventions: The first part of the name is NaCl*X*, where *X* is the millimolar concentration of NaCl in the simulation. The next part of the name refers to the temperature of the simulation, T*Y*, where *Y* is the temperature in Kelvin. For the CG simulations the water model used is indicated next in the name, with a W for the standard MARTINI water model and PW for the polarizable water model. The number of beads in the lipid tails is finally noted as "st" for short tails (one bead) and "lt" for long tails (two beads). For the atomistic simulations the name of the applied lipid force field is noted in the end of the simulation name instead. Hence, a simulation with the name NaCl150T310PWlt is carried out with a NaCl concentration of 150 mM, a temperature of 310 K, and by using the polarizable water model and a lipid representation with two beads in each lipid tail of DHPC.

Coarse Grained Simulations. All CG MD simulations in the current study have been carried out in the software package GROMACS 4.0.7[24] using the MARTINI CG force field version 2.1[9,25] and version 2.P.[26] Unless stated otherwise, all simulations are started from 1000 randomly oriented DHPC lipids, water beads, and ions (Na^+, Cl^-), giving rise to a lipid concentration of 200 mM. DHPC lipids are short tailed fully saturated lipid molecules with six carbon atoms in each fatty acid chain of the molecule. DHPC was not included in the original MARTINI paper[27] and to the best of our knowledge, no mapping of DHPC compatible with MARTINI has been

published. Since MARTINI generally maps four heavy atoms to one bead, DHPC may in principle be represented by either one or two beads in each tail. We have therefore tested both models (see Figure 1).

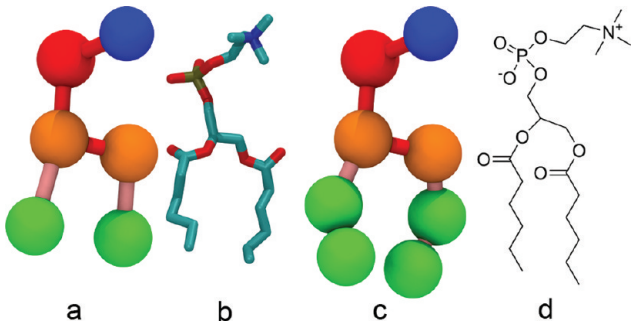

Figure 1. (**a**) CG DHPC with short tail representation. Beads are colored by their MARTINI type; Q_a-beads are red (mapping the phosphate group), Q_0-beads are blue (mapping the choline group), N_a-beads are orange (mapping the glycerol linker), and C_1-beads are green (mapping the aliphatic lipid tails). For a discussion of bead types, see ref 27. (**b**) AA representation of DHPC (hydrogens not shown). (**c**) CG DHPC mapped with the long tail representation using the same color code as in (**a**). (**d**) Chemical structure of a DHPC lipid molecule.

Two water models are available in the MARTINI force field. One is the standard water model (W) where four water molecules are mapped to one uncharged bead of polar type. This water model is therefore nonresponsive to electrostatic fields, which makes it impossible to model the polarization effect of real water and the screening of charges. This is compensated for by applying a relative dielectric constant of 15, which introduces an implicit screening on all Coulomb interactions. Recently, a polarizable water model (PW) for the MARTINI CG force field was published.[26] Here, a CG water bead still represents four water molecules, but now a water bead consists of three particles allowing for polarization of the water bead. Introducing the polarizable water to the model makes it possible to reduce the relative dielectric constant from 15 to 2.5.[26] We carried out simulations testing the performance of both water models with both mapping schemes of DHPC. To investigate the differences between the results obtained with the two CG water descriptions, simulations were constructed where the water model was changed after 2 μs of simulation, and additional 2 μs of simulation was undertaken with the other water model. The water model was changed by deleting the original water beads and then resolvating the lipids and ions with the other water model followed by an energy minimization of the resolvated lipid aggregates before restarting the MD simulation.

In simulations with nonzero NaCl concentration, the Na^+ and Cl^- ions are modeled as described in the MARTINI force field, using charged beads including the first hydration shell around the ions.[9] To maintain the same effective lipid concentration in all simulations, the number of water beads in the simulation setups therefore decreases when the NaCl concentration increases. Since the first hydration shell for both sodium and chloride ions contains six water molecules,[28] the number of water molecules in the different setups is increased by two when a water bead is replaced by an ion, hence for every second Na^+- and Cl^--ion an additional water bead was removed, except in the simulations with 150 mM NaCl (see Table 1), where the effect of extra water molecules is insignificant.

The systems were built by placing 1000 CG lipids randomly in a simulation box and solvating with water beads, either using the W or PW water model. The dimensions of the simulation boxes were deliberately made large enough to easily contain all the lipid, water and salt beads; however, after a few nanoseconds of simulation time the boxes had contracted to reach a common side length (for all three dimensions) of around 20−21 nm for the remainder of the trajectory in all simulations. Ions were added to the system by the "genion" program from GROMACS,[24] and the system was energy minimized in 500 steepest descent steps. For the production runs a Lennard-Jones cutoff of 1.2 nm was used with shifting starting from 0.9 nm.[9] Also, the Coulomb potential was shifted to zero with the GROMACS shift-function in the interval from 0.0 to 1.2 nm.[9]

In all CG simulations an isotropic pressure coupling was used with a target pressure of 1.0 bar. Both the pressure and the temperature were controlled by the Berendsen weak coupling algorithm[29] with time constants τ_T = 0.1 ps, τ_P = 0.5 ps, and a compressibility of $1{\cdot}10^{-5}$ bar^{-1} for simulations with standard water and τ_T = 0.3 ps, τ_P = 3.0 ps, and a compressibility of $3{\cdot}10^{-5}$ bar^{-1} for simulations with polarizable water. The temperature was varied between 285 and 323 K. For the simulations with standard water a time step of 40 fs was applied. For the simulations in polarizable water a time step of 25 fs was used, and all simulations were run for 2 μs. In CG simulations, the heavier bead-particles make the energy surface smoother and accelerate the dynamics. It has been shown that the simulated time typically should be multiplied by a factor of 4 to roughly account for the increase in diffusion observed for CG water beads.[9,27] However, throughout this paper we will refer to the actual simulation times, not applying this multiplication.

Reverse Coarse Graining. The rvCG simulations were set up by isolating eight micelles from the last snapshot of the CG simulation named NaCl150T298PWst and adding enough free lipids (eight) to the simulation box (~12 × 12 × 15 nm) at random positions and orientations, to make the free lipid concentration the same as observed during the CG simulation. The lipids were converted to an atomistic description using either GROMOS96 or CHARMM36 as described below, and water and ions were added prior to the simulated annealing process.

Atomic Resolution Micelles with GROMOS Parameters. To convert the identified CG micelles into a united atom (UA) description, the rvCG script described by Rzepiela et al.[30] was used. Here, a mapping of the CG molecules to their UA representation is provided to the algorithm. A simulated annealing protocol was then carried out, making it possible for the molecule to cross large energy barriers and relax the UA structure, while restraints ensured that the final UA structure belonged to the structural ensemble represented by the starting CG structure.[30] The simulation conditions were the same as reported by Rzepiela et al.[30] For the simulation named NaCl150T298Kukol, the topology for DHPC was created by simply removing 10 methylene groups from each chain of the 1,2-dipalmitoyl-*sn*-glycero-3-phosphocholine (DPPC) topology, as described by Jiang et al.[10] The GROMOS96 53A6 parameter set[31] together with the lipid parameters adjusted by Kukol[13] were applied in the simulated annealing as well as the production run. For the simulation named NaCl150T298Berg-

er, the DHPC topology was constructed by removing 8 methylene groups from each chain of the 1,2-dimyristoyl-*sn*-glycero-3-phosphocholine (DMPC) topology, and the production run was started from the same rvCG structure as for the NaCl150T298Kukol simulation and applied the lipid parameters developed by Berger[32] within the GROMOS96 53A6 force field.

The simulation parameters were identical to those used for the CG simulations, except that the electrostatic interactions were described with a Particle Mesh Ewald (PME)[33] method, and the temperature and pressure were kept constant via a Berendsen thermostat and barostat[29] with time constants of τ_T = 0.1 ps and τ_P = 1.0 ps and a compressibility of $4.5 \cdot 10^{-5}$ bar^{-1}. The target temperature and pressure were set at 298 K and 1.0 bar, respectively, and the lipids were solvated using the SPC water model.[34] All bonds were constrained by the LINCS algorithm,[35,36] a time step of 2 fs was used and the simulations were run for 100 ns.

Atomic Resolution Micelles with CHARMM Parameters. A similar conversion from the CG description of the DHPC micelles to AA using CHARMM36 was done by use of the CGTools Plugin in VMD[37] with residual based coarse graining,[38,39] and simulations were run with the CHARMM36[40] force field in NAMD 2.7.[41] Following an initial energy minimization, a simulated annealing procedure was carried out during which the centers of masses of the atom groups corresponding to the mapped beads were restrained to the position of their respective beads. The temperature started at 610 K and was decreased by 10 degrees every 500 steps until it reached 300 K. A time step of 1 fs was used. The nonbonded short-range interactions were updated every time step, while full electrostatics PME was calculated every second time step and pair lists were updated every 10 steps. A switching function was used for the short-range nonbonded interactions starting at 10 Å with a cutoff at 12 Å, and the pair list distance was set to 13.5 Å (CGTools default). The TIP3P water model[42] was used with water bonds constrained. Finally, the system was energy minimized before the production run. The production run had the same simulation parameters as the simulated annealing except that the short-range nonbonded interactions were updated every second time step, full electrostatics was calculated every fourth time step, and pair lists were updated every 20 steps. Furthermore, the pair list distance was set to 14 Å. The target temperature was set to 298 K and controlled by a Langevin algorithm with a damping constant of 5 ps^{-1}. The target pressure was set to 1.01325 bar and controlled by a Nosé-Hoover Langevin piston[43] with a period of 100 fs and a decay of 50 fs. The simulation was run for 100 ns using a time step of 1 fs.

Analyzing Lipid Aggregates. All CG MD simulations were found to have reached a stable level of aggregation after 1 μs of simulation as evaluated from aggregation number distributions measured at 0−0.5, 0.5−1.0, 1.0−1.5, and 1.5−2.0 μs (see Figure S1 in the Supporting Information), and all analyses were therefore carried out on the last microsecond of the 2 μs simulations, using a total of 890 evenly distributed frames. Similarly, the analyses of the aggregates in the AA/UA MD simulations were carried out over the last 50 ns of the 100 ns simulations, using a total of 1000 frames.

Lipids were defined as belonging to the same aggregate if they had either the beads describing the hydrophobic tails or the glycerol linker closer than 6 Å to each other in the CG simulations. The lipid headgroup was excluded from the definition to avoid counting neighboring micelles as one. This criterion was established based on visual inspection, and the results were not found to be particularly sensitive to the choice of distance; any threshold between 5 and 7 Å leads to very similar groupings of the lipids. For the AA simulations the same limit was applied, and lipids were defined as belonging to the same aggregate if they had atoms from the hydrophobic tails including the glycerol linker closer than 6 Å to each other. For the evaluation of the free lipid concentration, a lipid was defined as free if it participated in an aggregate with at most five lipids. This limit was determined based on the distribution of aggregation numbers collected from a CG simulation where micelles comparable to experimental observations were formed (see Figure S2**a** in the Supporting Information). For the CG simulations Gaussian functions were fitted to the part of the aggregation number distributions corresponding to aggregates. If a fit of reasonable quality could be made, the center of the fit and the standard deviation are given as the average aggregation number for the simulation, and also the *R*-value of the fit is given. For the simulation named NaCl500T298PWst a reasonable fit could only be obtained as a sum of two Gaussians, and in this case the center and standard deviation for both Gaussians are listed. All Gaussian fits can be seen in Figure S2 in the Supporting Information. For the atomic resolution simulations the aggregate size distributions do not reach equilibration within the 100 ns of simulation time. The listed aggregation numbers are therefore plain averages with standard deviations and not based on Gaussian fits. The size of an aggregate was established from its extension along the principal axes of inertia. The shapes of the aggregates were divided into three types as illustrated in Figure 2. A lipid aggregate was classified as oblate if the difference between the two largest dimensions was smaller than the difference between the two shortest dimensions. Similarly, a prolate topology was assigned if the difference between the two shortest dimensions was smallest. If the differences between the shortest and largest dimensions were both smaller than 6 Å, the aggregate was classified as spherical.

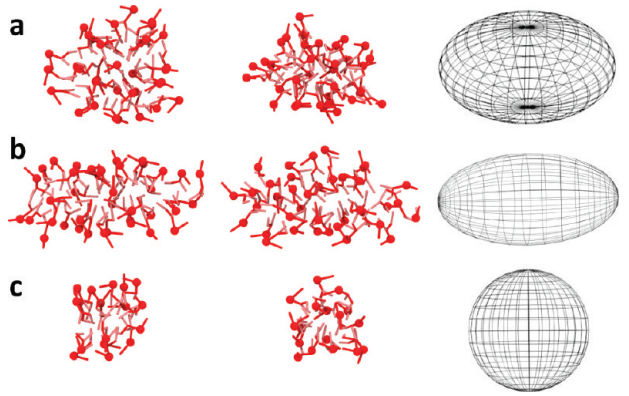

Figure 2. Micelle topologies illustrated by a representative aggregate shown as "top-view" in column one and "side-view" in column two, as well as a schematic representation in column three: **a**) an oblate micelle, **b**) a prolate micelle, and **c**) a spherical micelle.

Simulation Overview. The 16 simulations carried out in this study are listed in Table 1, specifying the conditions used in each simulation. Four simulations were constructed to test the effect of mapping the aliphatic lipid tails in the CG description of DHPC with either one or two beads, referred to as short tails

Table 2. Average Aggregation Numbers for DHPC Micelles as Found From Experiments

source	aggregation number	lipid concentration[a]	conditions[b]	method
Lipfert et al.[44]	25−40[c]	≤50 mM	T = 298 K, salt: 150 mM NaCl	SAXS
Chou et al.[14]	27	≤442 mM	T = 300 K, salt: 5 mM azide	NMR
Lin et al.[21]	19	27−361 mM	temperature not specified	SANS[d]
Tausk et al.[16]	35	15−42 mM	T = 297 K, salt: 0−3 M NaCl	light scattering and ultracentrifugation data

[a]The concentration at which the reported aggregation number was found. [b]The conditions under which the experiment was conducted. In addition all experiments also included phosphate buffer. [c]A range is reported since different techniques were applied in the analysis of the data. [d]Small Angle Neutron Scattering.

(st) or long tails (lt). Four simulations were performed to test the effect of using the polarizable water model instead of the standard MARTINI water model. Two extra simulations were carried out to explore the effect of changing the NaCl concentration. Three more simulations investigated the influence of the temperature on the micelles, and finally three rvCG simulations were done to compare different atomistic force fields with respect to describing stable micelles.

RESULTS AND DISCUSSION

The analysis of the MD simulations will focus on two parameters measured experimentally several times for DHPC micelle solutions: the CMC of DHPC, which corresponds to the free lipid concentration when the total lipid concentration is above the CMC, and the average number of DHPC lipids forming a micelle (the aggregation number). Apart from this, the observed topology of the lipid aggregates is evaluated and compared to those observed in experiments. For DHPC lipids in solution with 0−0.1 M NaCl the CMC is found in the range 11−16 mM depending on the method used.[14−23] Furthermore, DHPC micelle solutions are monodisperse[16,44] or only polydisperse to a small degree,[21] but the average aggregation number is found to vary considerably, as values between 19 and 40 DHPC lipids per micelle have been reported for different experiments (see Table 2). Small Angle X-ray Scattering (SAXS) experiments have revealed the structure of DHPC micelles to be best described as prolate spheroids,[21,44] where the short dimension is found to be 25−36 Å and the long dimension to be 47−60 Å. However, it is not clear to what degree these measures include hydration of the lipid head groups.

The progression of this section is as follows: First two options of CG DHPC tail length representation are tested as well as two different MARTINI water models. Then the water model choice is further examined to exclude possible effects from bias in the initial setups. Having concluded on the optimal choice of CG representation for the system, it is then investigated if the expected response to changes in salt concentration and temperature can be described within the optimal CG model. Finally, a selection of eight micelles are reverse coarse grained, and simulations are carried out using three different atomistic resolution force fields to explore the ability of these models to describe DHPC in dynamic lipid aggregates.

CG Representation of Lipid and Water. The standard way to map a phosphatidylcholine (PC) lipid in the MARTINI CG force field is by taking DPPC, which has been thoroughly parametrized, and cut off tail beads until the number of beads corresponds to the number of carbon atoms in the studied lipid tails.[9] However, as the CG model maps four methylene groups to a single bead, it is only possible to make a straightforward representation of alkyl chains with a multiple of four carbons in the fatty acid chains. When representing DHPC we therefore have a choice between mapping to one or two beads per lipid tail (see Figure 1). PC lipids with two-beaded lipid tails (to model dicapryloyl-PC) have previously been shown to form a network of wormlike micelles when starting from a bilayer setup at T = 325 K and using the standard water model.[9] The lack of independent micelle formation is in this case accredited to the high lipid concentration in the simulation. The length of the lipid tails affects the headgroup-to-tail size ratio, and the lipid tail mapping will therefore have an effect on the amphiphatic properties of the lipids and thus on the aggregation propensity.

The standard water representation in MARTINI is an uncharged polar bead representing four water molecules. In 2010, a refined water model was presented,[26] allowing for polarization of the water bead upon interaction with charged beads. To inspect the sensitivity of the CG setup to the choice of lipid tail length and water model, simulations were set up with the four combinations of system representation (see Table 3).

Table 3. Simulations with DHPC Described with Short (One Bead) or Long (Two Beads) Tails and with the Standard or Polarizable Water Model

simulation name	free lipid concentration [mM]	aggregation number	structure[b]
NaCl0T298Wst	2.9 ± 0.7	not available[a]	long bending worms
NaCl0T298PWst	9.5 ± 1.5	24 ± 7 (R = 0.97)	18% S, 60% P, 22% O
NaCl0T298PWlt	0	not available[a]	13% S, 42% P, 45% O[c]
NaCl0T298Wlt	0	not available[a]	0% S, 0% P, 100% O[d]

[a]Aggregates were too few to allow for a meaningful Gaussian fit. [b]Aggregate structures divided in spherical (S), prolate (P), and oblate (O) topologies if possible. [c]The distribution of shapes is not equilibrated; the amount of spherical micelles continuously decrease over the simulation time. [d]Three bicelles are formed which stay unchanged for the last microsecond of the simulation.

It is seen that the size and topology of the formed lipid aggregates vary considerably in the four simulations. Examples of the formed aggregates are shown in Figure 3. When DHPC is represented with one-beaded tails and combined with the standard water model, the aggregation process results in long branched wormlike structures. However, when the polarizable water model is used, the DHPC lipids with one-beaded tails form micelles. Using the two-beaded mapping of the fatty acid chains of the DHPC lipids, the aggregates formed are either disk shaped or exhibit a clearly nonspherical symmetry in the case of standard water environment or form bilayer ribbons and

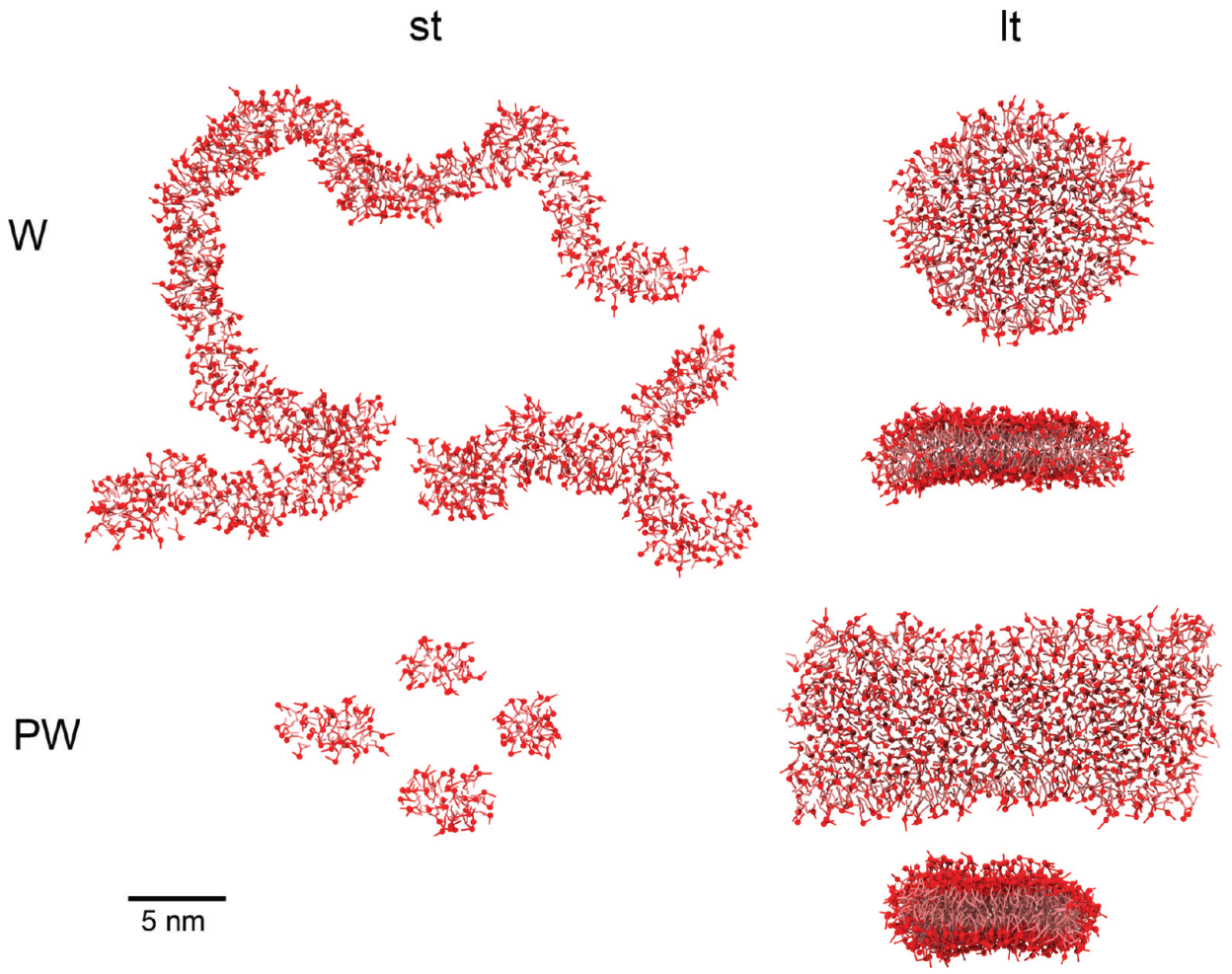

Figure 3. Characteristic examples of aggregates from the simulations using the standard water model (top row), polarizable water model (bottom row), one-beaded short tails (left column), and two-beaded long tails (right column − showing both top and side views). Phosphate beads (Q_a bead type) are shown as red spheres, while the rest of the lipid is shown with sticks.

smaller discs when combined with the polarizable water model. Both of these latter types of aggregates are as expected from more hydrophobic lipids with longer fatty acids than those present in DHPC.[9,45]

Judging solely from the topology of the aggregates, the lipids with two-beaded tails hold too much hydrophobicity to represent the amphiphatic nature of DHPC in a satisfactory manner. Also, the branched wormlike structures observed when lipids with one-beaded tails aggregate in the standard water model are not characteristic of the DHPC aggregates observed experimentally.[21,44] However, when the lipids with one-beaded tails self-assemble using the polarizable water model, micelles of different sizes are formed in accordance with experiments. The micelles are found to be mainly prolate in shape, and with an average aggregation number (24 ± 7) within the experimentally observed range (19−40).[14,16,21,44] Based on the free lipid concentrations measured in the simulations (see Table 3) it is also seen that the polarizable water model together with the short tailed lipids allows for a much better description of the equilibrium between aggregated and free DHPC lipids than does the standard water model.

These simulations thus suggest that the short tailed lipid mapping should be chosen together with the polarizable water model. Through the rest of this paper the DHPC lipid mapping with one-beaded tails is therefore used, while the choice of water model is inspected in greater detail in the following section before making the final recommendation.

A Closer Look at the CG Water Model. To make sure that the remarkable effects observed based on the chosen water model may neither be caused by biases in the initial setup nor be due to the absence of NaCl in the solution, new simulations were set up, this time adding Na^+ and Cl^- ions to a concentration of 150 mM, see Table 4. The addition of salt

Table 4. Lipid Aggregation Before and After Switch of Water Model

simulation name	free lipid concentration [mM]	aggregation number	structure[b]
NaCl150T298PWst	7.1 ± 1.2	26 ± 8 (R = 0.99)	14% S, 65% P, 21% O
NaCl150T298Wst	3.0 ± 0.7	not available[a]	long bending worms
W-NaCl150T298PWst	2.9 ± 0.7	not available[a]	long bending worms
PW-NaCl150T298Wst	7.3 ± 1.2	27 ± 9 (R = 0.97)	13% S, 67% P, 20% O

[a]Aggregates were too few to allow for a meaningful Gaussian fit. [b]Aggregate structures divided in spherical (S), prolate (P), and oblate (O) topologies if possible.

dx.doi.org/10.1021/ct200921u | J. Chem. Theory Comput. 2012, 8, 1556−1569

did not cause any noticeable changes in the formation and structure of the lipid aggregates, and as before, long branched worms were formed in the simulation using the standard water model, whereas micelles resulted from the simulation with the polarizable CG water model. Then, to make a strong test against effects from any initial bias of the simulation setup, the lipid aggregates formed after 2 μs of simulation were resolvated with the other water model such that the aggregates that were formed using the standard water model now were placed in a polarizable water environment and *vice versa*; see entries W-NaCl150T298PWst and PW-NaCl150T298Wst in Table 4. These setups with interchanged water models were then run for an additional 2 μs.

In Figure 4**a**, the number of independent lipid aggregates as a function of simulation time is depicted. As the aggregates keep

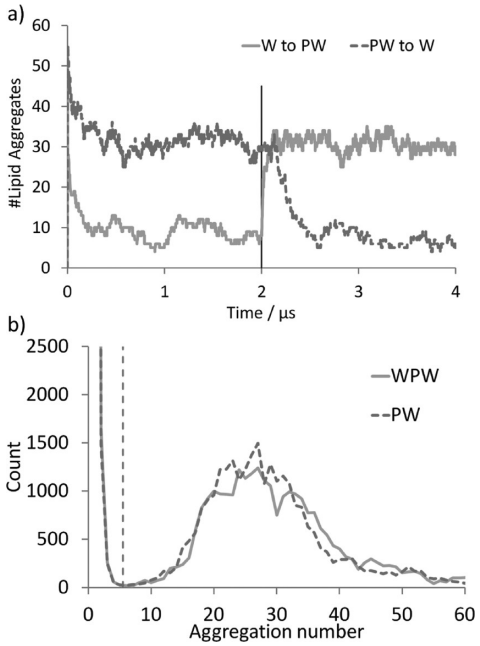

Figure 4. The effect of the water model choice on the aggregation. **a**) Number of lipid aggregates (independent micelles) as function of time. The free lipids (aggregates containing five or less lipids) have been excluded from the graph. Simulations started from random with polarizable water (dashed dark gray line) and standard water (solid light gray line). After 2 μs of simulation the water model was changed from polarizable water to standard water and *vice versa* (marked by a vertical line). **b**) The distribution of aggregation numbers for the observed aggregates measured from 1 to 2 μs in the simulation NaCl150T298PWst starting with polarizable water (PW) and from 3 to 4 μs in the simulation PW-NaCl150T298Wst starting with standard water but changing water model after the first 2 μs (WPW). Aggregates left of the broken vertical line are counted as free lipids.

fusing and dividing during the simulation time, the number of aggregates keeps varying. It is therefore not easy to state explicitly when the aggregation process has reached equilibrium. Still, for both water models the number of aggregates appears to have converged to the final level after approximately 500 ns. As the results listed in Table 4 are evaluated from the last microsecond of the simulations it can be assumed that the equilibration phase of the self-assembly process is left out of the analyses. From the aggregate size distribution resulting from the simulation with the polarizable water model (Figure 4**b**, PW) it is clear that a monodisperse solution is obtained as expected from experiments; however, the size distribution is not completely smooth. Although aggregates can be formed within 10−100 ns of CG simulation,[46] the following diffusion is very slow,[10] and it could be argued that a longer simulation time would lead to a fully equilibrated and more narrow size distribution of the lipid aggregates. However, comparing the aggregate size distribution collected from 0.5 μs−1 μs with the distributions collected from 1 to 1.5 μs and 1.5 to 2 μs (Figure S1 in the Supporting Information), no trend pointing to a narrowing of the size distribution is observed, even though lipids easily exchange between aggregates at this time scale. Based on these observations we estimate that the simulation time of 2 μs is sufficient to describe the general trends of DHPC micelle equilibrium properties within our model.

When the water model is changed after 2 μs of simulation, an abrupt adjustment in the number of lipid aggregates is seen (Figure 4**a**). The few large aggregates formed in the standard water model quickly dissolve to smaller micelles resulting in the observed immediate increase in the number of aggregates. The micelles formed with the polarizable water model start fusing as soon as the water model is changed to the standard model, and a decrease in the number of aggregates is observed until it levels off at the same number of aggregates as was observed in the simulation starting from a random distribution of lipids and using the standard water model. It is also seen from Table 4 that the effect of using polarizable water compared to standard water is completely reversed for the free lipid concentration, the aggregation number and the diversity of aggregate topologies. It is thus evident that the water model directly affects the lipid aggregation and that the results were not biased in any way by the building procedure.

The lipid aggregates obtained from the simulations using the standard water model predominantly have wormlike topologies, containing a large number of lipids (Figure 3, upper left corner). Other topologies can also be observed such as small spherical, prolate, and oblate micelles, but they are formed by a small fraction of the lipids. Micelles formed when using the polarizable water model are found to be spherical or slightly prolate/oblate with a diameter of 34 ± 3 Å and a length of 47 ± 8 Å, see Figure S3 in Supporting Information, which is in excellent agreement with the size of DHPC micelles found experimentally.[14,21] Only a few longer prolate structures are observed with a length above 70 Å. With both water models micelles can be observed to change from a prolate to an oblate structure and *vice versa* during the simulation. These fluctuations between topologies can be attributed to the thermal fluctuations of the system that allows the micelles to overcome the small energy barriers between the different aggregate shapes.

The simulations with the polarizable water model result in higher free lipid concentrations (∼10 mM without NaCl and ∼7 mM at 150 mM NaCl) which is closer to the experimentally observed 11−16 mM than the ∼3 mM concentration obtained when using the standard water model. That MARTINI with the standard water model under-predicts the CMC/free surfactant concentration has previously been noted by Sanders et al.[47] as they found the free surfactant concentration of dodecylphosphocholine (DPC) to be 2 orders of magnitude off. The increase in the free lipid concentration observed when using the polarizable water model is not surprising as lipid or surfactant monomers are stabilized by both the introduction of directional electrostatic interactions to water beads and the 10% lower energy barrier for moving a C1-bead from a hexadecane to a

water phase.[26] These changes to the MARTINI model combined with a significant decrease in the relative dielectric constant (from 15 to 2.5) and adjustments of the Lennard-Jones interactions for charged beads all affect the aggregation preference of the DHPC lipids and explain the distinctive differences in aggregation topology following the choice of water model.

Another notable difference between the simulations in polarizable and standard water is that the charged headgroup beads of lipids belonging to different aggregates can be observed at interbead distances as short as 4.7 Å when using the polarizable water model, which is never observed in the simulations using the standard water model. The same effect was reported for sodium and chloride ions by Yesylevskyy et al.[26] This difference in the packing of opposite charges may simply be caused by the decrease in implicit charge screening when using the polarizable water model[26] and, as noted by Yesylevskyy et al., it is difficult to comment on the correctness of this behavior.

In previous MARTINI simulations of lipid bilayers[26] and the surfactant cetyltrimethylammonium chloride,[48] the lipid aggregate structures were reported to be practically unaffected by the choice of water model. However, in both cases the aggregates were preassembled, and in the case of the surfactant, the molecules formed a single micelle, leaving it unanswered if two spherical micelles or a wormlike structure would form if the number of surfactant molecules was increased. The results presented here demonstrate that even though for some CG MD modeling studies the standard water model will provide a satisfactory description of the solvent phase, the polarizable model introduces a clear improvement and it is hard to predict when the standard model will suffice.

As we have now thoroughly established that the polarizable water model is essential for obtaining a satisfactory description of the short-tailed lipid DHPC in water, this water model is used in all CG setups for the rest of the study. In the following sections we investigate if the expected response to changes in NaCl concentration and temperature can be described equally well within this CG model for DHPC micelle solutions.

NaCl Concentration Effects. It has been found experimentally that changes in NaCl concentration can affect both the CMC and the aggregate topology of surfactants.[49−52] Specifically for DHPC lipids it has been observed that the CMC decreases when the NaCl concentration increases,[53] which has been explained as the salting-out of the free monomers in the solution.[54] Apparently, this only has a small effect on the size of the micelles, increasing the measured micellar weight by only ∼6% going from no salt to a 1 M NaCl solution.[16] To test if these observations can be reproduced with the CG model of DHPC established in the previous sections, simulations were set up where only the NaCl concentration was varied, and the results are shown in Table 5.

When inspecting the structure of the aggregates it is evident that the size of the aggregates is affected by the salt concentration in the solution, contrary to what was found experimentally.[16] This is reflected in the average aggregation numbers listed in Table 5 and in the aggregate examples depicted in Figure 5. The majority of the micelles in the simulations with 0, 150, or 500 mM NaCl can be characterized as prolate spheres. The smaller micelles are mainly spheres, and the larger micelles are short worms which at the highest tested salt concentration develop into branched wormlike structures as illustrated in Figure 5**d**. Also, it is well-known that salt can induce sphere to rod transition in micelles of cationic surfactants,[50,51] and despite the zwitterionic nature of DHPC, this tendency is also seen from the topology analysis in Table 5, where the ratio of spherical versus prolate structures is shifted toward the prolate as the salt concentration is raised. It is a clear trend in our simulations that the structures get larger when the salt concentration is increased; however, two things should be noted in this regard. First, we should be aware that the simulation with 1000 mM NaCl is on the limit of what has been tested in the parametrization of MARTINI.[27] Second, even though the distribution of aggregate sizes is shifted toward higher aggregation numbers as the salt concentration is raised (see Figure 6**a**), the main difference is that a number of wormlike micelles with significantly higher aggregation

Table 5. Lipid Aggregation as the NaCl Concentration Is Varied

simulation name	free lipid concentration [mM]	aggregation number	structure[b]
NaCl0T298PWst	9.5 ± 1.5	24 ± 7 (R = 0.97)	18% S, 60% P, 22% O
NaCl150T298PWst	7.1 ± 1.2	26 ± 8 (R = 0.99)	14% S, 65% P, 21% O
NaCl500T298PWst	4.0 ± 1.0	30 ± 8 60 ± 22 (R = 0.94)	7% S, 77% P, 16% O
NaCl1000T298PWst	2.1 ± 0.7	not available[a]	long bending worms

[a]Aggregates were too few to allow for a meaningful Gaussian fit. [b]Aggregate structures divided in spherical (S), prolate (P), and oblate (O) topologies if possible.

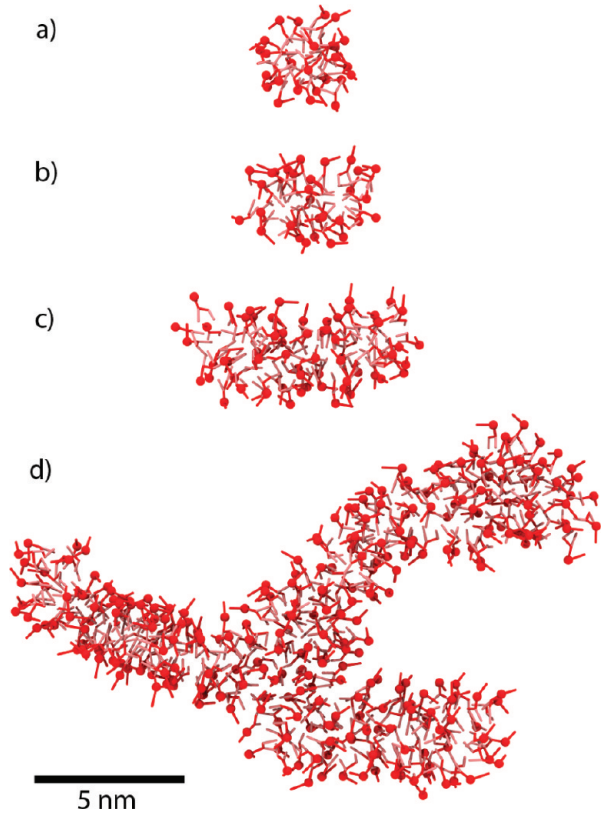

Figure 5. Representative aggregates observed after 2 μs of simulation in solutions with the following NaCl concentrations: (**a**) 0 M, (**b**) 150 mM, (**c**) 500 mM, and (**d**) 1000 mM.

dx.doi.org/10.1021/ct200921u | J. Chem. Theory Comput. 2012, 8, 1556−1569

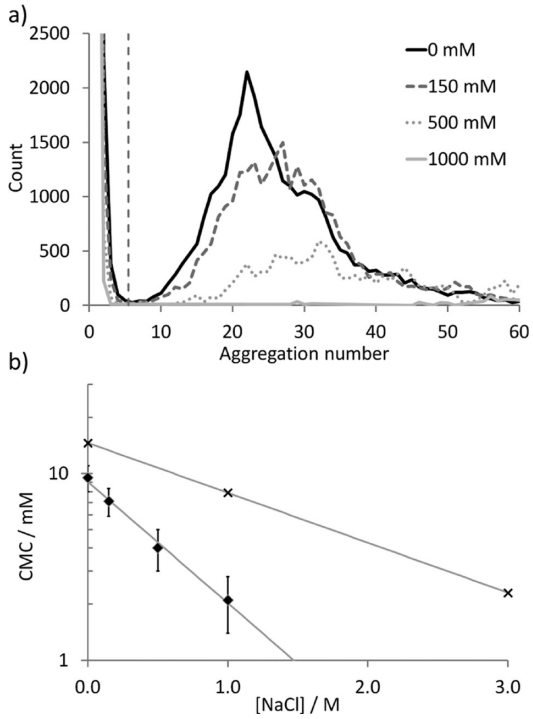

Figure 6. a) The distribution of aggregation numbers for the observed aggregates at different NaCl concentrations. Aggregates left of the broken vertical line are counted as free lipids. **b)** Log-plot of the CMC/free lipid concentration as a function of the NaCl concentration. Values from the simulations are shown as diamonds with standard deviations shown as error bars. Experimental values from Tausk et al.[53] are shown as crosses. Both data sets are fitted to a salting-out model; $\log\mathrm{CMC} = -k_s\,[\mathrm{NaCl}] + (\log\mathrm{CMC})_{[\mathrm{NaCl}]=0}$. k_s is a constant which depends on the type of salt studied,[53] and it is evaluated to 0.65 M^{-1} from the simulations and to 0.27 M^{-1} from the experiments.

numbers are starting to form at 500 mM salt concentration. Still, if the simulation with 1000 mM NaCl is disregarded, the majority of the micelles have aggregation numbers in the range of 20−45 at all the tested salt concentrations.

The average free lipid concentrations for the DHPC lipids in the four simulations listed in Table 5 are plotted as a function of the salt concentration in a log-plot in Figure 6**b**. The CMCs measured by Tausk et al.[53] are also included in the plot, and it is clear that the free lipid concentration observed in the simulations decreases as the salt concentration is increased, equivalent to what has been measured in the experiments. Both the experimental CMC and simulated free lipid concentration values fit perfectly with the salting-out model from Tausk et al.[53] as illustrated by the linear trend line. As the slope of the trend line is higher for the simulated free lipid concentration values, this shows that the salting-out effect is exaggerated in the simulations and would probably lead to a solution without free DHPC lipids at a salt concentration around 1.5 M. As other problems with the CG model would show up at such a high salt concentration this is not a major concern.

Based on these results, the CG model behaves satisfactory when simulating in the 0−500 mM range of salt concentrations. Even though the free lipid concentration throughout this range is around 5 mM lower than observed experimentally, the shift in equilibrium is reproduced, and the formed aggregates are within the expected size and topology.[14,16,21,44] It can however not be recommended to go for higher salt concentrations as effects contrary to what has been reported experimentally appear, resulting in branched wormlike structures in the 1000 mM NaCl solution.

Temperature Effects. The effect of temperature on the CMC of DHPC has also been investigated experimentally, and van Dam et al.[55] find that within the tested temperature range of 288 K−318 K, the free lipid concentration is practically unaffected. The effect of temperature on the size of micelles has furthermore been found to be minor, with a slight decrease of the aggregation number with increasing temperature for a zwitterionic surfactant.[56] To study the temperature effects on our modeled system, we set up four simulations with different temperatures ranging from 285 K to 323 K (see Table 6). The MARTINI force field has been parametrized using temperatures between 270 K and 330 K so the simulations are well within these limits.[9,27]

Table 6. Lipid Aggregation as the Temperature Is Varied

simulation name	free lipid concentration [mM]	aggregation number	structure[a]
NaCl150T285PWst	4.0 ± 1.0	29 ± 10 (R = 0.94)	11% S, 69% P, 20% O
NaCl150T298PWst	7.1 ± 1.2	26 ± 8 (R = 0.99)	14% S, 65% P, 21% O
NaCl150T310PWst	12.3 ± 1.7	24 ± 7 (R = 0.99)	17% S, 62% P, 21% O
NaCl150T323PWst	20.6 ± 2.3	21 ± 7 (R = 0.99)	19% S, 59% P, 22% O

[a]Aggregate structures divided in spherical (S), prolate (P), and oblate (O) topologies.

When inspecting the average aggregation numbers, it is seen that there is a trend toward smaller aggregates with increasing temperature. However, the means of the distributions are comparable within the standard deviations, and all are within the range of experimentally determined values for the aggregation number. Also, when studying the aggregates in the simulations visually, the effect from raising the temperature is mainly seen as a minor increase in the population of spherical micelles, which are the smallest aggregates, at the expense of small prolate spheroid ones. Thus, these results, showing only little temperature effect on the lipid aggregate's size and topology, are in accordance with experimental observations[56] for the temperature range studied here.

In Figure 7**b** the free lipid concentration is plotted as a function of the inverse temperature. It is evident that there is a perfect linear relation between log(CMC) and $1/T$, as also observed previously in a study of MARTINI CG surfactant solutions.[47] Both in the case of DHPC lipids studied here and for the surfactants studied by Sanders et al.,[47] an increase in free lipid concentration is observed for higher temperatures, even though experimental CMCs for the surfactants either remain practically constant or decrease. Sanders et al. obtain CMC values for the zwitterionic surfactant DPC which are underpredicted by 2 orders of magnitude,[47] and they speculate that the discrepancy is mainly due to the unstructured solvent model not being able to simulate hydrogen bonding between the water molecules. We would therefore expect to see significantly improved results when using the polarizable water model in MARTINI. However, even though we observe a clear improvement in the free lipid concentration going from standard water (free lipid concentration ∼3 mM) to polarizable water (free lipid concentration ∼10 mM), it is unlikely that this

dx.doi.org/10.1021/ct200921u | J. Chem. Theory Comput. 2012, 8, 1556−1569

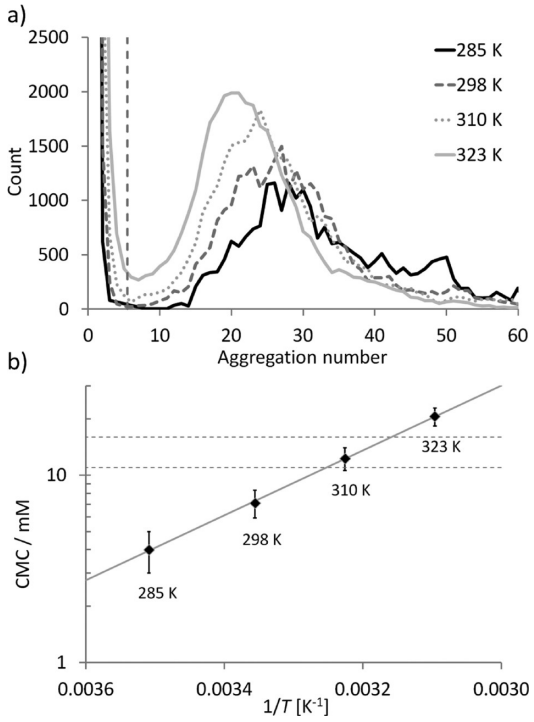

Figure 7. a) The distribution of aggregation numbers for the observed aggregates at different temperatures. Aggregates left of the broken line are counted as free lipids. **b)** Log-plot of the free lipid concentration (CMC) as a function of the inverse temperature − notice the $1/T$ scale is reversed. Values obtained from the simulations are shown as diamonds with standard deviations shown as error bars. A linear fit to the points has been made, illustrating the relation $\ln(\mathrm{CMC}) = \Delta G/kT$ where k is Boltsmann's constant and ΔG is the Gibbs free energy change on micellization,[57] which in this case is −33 kJ/mol. The horizontal dashed lines indicate the extremes of experimentally measured CMCs for DHPC.[18]

effect from the polarizable water model would be great enough to alter the DPC monomer-micelle equilibrium by 2 orders of magnitude. The main difference between CG DHPC and CG DPC is the hydrophobic/hydrophilic bead ratio, and this is probably the reason for the better modeled free lipid concentration values obtained for DHPC in both the standard and polarizable water model.

As the variation in temperature produce free lipid concentration values of the right order of magnitude without changing the topology of the aggregates significantly, the temperature could be set in the simulation to produce a particular free lipid concentration value if this property was important for the model to be applicable. The experimentally established CMC is around 11−16 mM at zero or low salt concentration and should be somewhat lower at a salt concentration of 150 mM NaCl, as is the case for these simulations. Choosing a simulation temperature of around 310 K would thus produce a free lipid concentration similar to what appears from experimental data. Another benefit from simulating at a higher temperature is that fully equilibrated aggregate distributions are more easily achieved as witnessed by the distribution curves getting smoother with increased temperature in Figure 7a. However, changing the temperature can have unforeseen effects on other properties of the system, and in the light of other approximations made when using CG modeling, the exact match with a CMC value would seldom be critical. If it is sufficient that the model reproduces a CMC of the right order of magnitude, the temperatures tested here are all acceptable.

Micelle Aggregates at Atomistic Resolution. It is extremely valuable to combine the microsecond time scale accessible with CG MD simulations with the high spatial resolution in atomistic MD. To this end we have carried out rvCG simulations of a selection of the self-assembled micelles obtained from the CG MD simulations, to evaluate the performance of three different atomistic force fields in reproducing DHPC micelles with properties similar to experimental observations. Eight micelles were isolated from the last frame of the NaCl150T298PWst simulation (see Table 1), and eight free lipids were added to match the free lipid concentration found in the CG simulations (see e.g. Table 4). The resulting molecular assembly was then reverse coarse grained and resolvated with all-atom water molecules. This procedure was used for three 100 ns simulations with different force fields; namely the most recent CHARMM36 lipid parameters,[40] the so-called Berger lipids[32] which is based on parameters constructed by combining bonding term parameters from GROMOS96 with nonbonding parameters from OPLS,[58] and a modification to the GROMOS96 53A6 parameter set[31] for PC lipids presented by Kukol.[13]

The free lipid concentration evaluated as an average over the last 50 ns of the simulations are listed in Table 7 and seen as a function of simulation time in Figure 8a. For the simulations applying CHARMM36 or Berger lipids, the underestimation of free lipid concentration seen for the CG simulation is alleviated, and the modeled free lipid concentration is here in line with what has been observed experimentally. Still, within the simulation time large fluctuations are seen, arising from the hard cutoff definition of when a lipid molecule is considered free, but also caused by the small number of lipids needed to change the free lipid concentration significantly. Since the number of lipids in the system is small (N = 233 and [DHPC] = 200 mM), the free lipid concentration changes by ∼1 mM when a single lipid either dissociates from or associates with a micelle. It is not obvious whether the variations in free lipid concentration with time are due to fluctuations around equilibrium or if it is due to the free lipid concentration not having reached equilibrium within the 100 ns. No matter which, it is clear that the free lipid concentration is increased compared to the CG simulations. Furthermore, the free lipid concentration obtained using the Kukol parameters stands out, showing a decrease in free lipid concentration as compared to the already slightly too low free lipid concentration resulting from the CG simulations. The distinctive difference between

Table 7. Simulations with DHPC Described with Different Atomistic Lipid Parameters

simulation name	free lipid concentration [mM]	aggregation number	structure
NaCl150T298CHARMM	16.3 ± 3.1	40 ± 17	multiple micelles
NaCl150T298Kukol	3.1 ± 1.1	>233[a]	single aggregate
NaCl150T298Berger	13.1 ± 2.8	44 ± 17	multiple micelles

[a]The calculated mean is 229 ± 7, but as the setup only includes 233 lipids, this indicates that the aggregation number is probably higher than the number of lipids in the simulation.

dx.doi.org/10.1021/ct200921u | J. Chem. Theory Comput. 2012, 8, 1556−1569

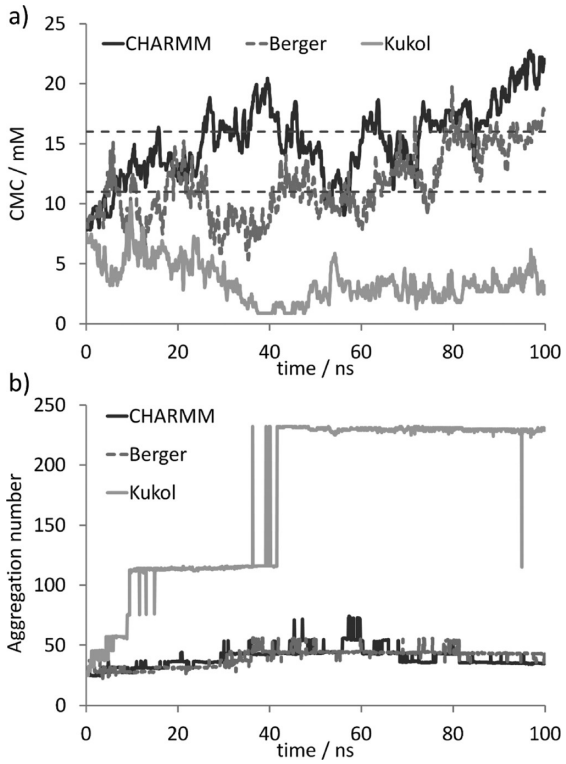

Figure 8. Results from the rvCG simulations using three different atomistic lipid force fields. **a**) Free lipid concentration (CMC) found in 2000 snapshots evenly distributed over the 100 ns simulation time. Running average over five snapshots are shown. Horizontal dashed lines indicate the extremes of experimentally measured CMCs for DHPC.[18] **b**) Mean aggregation number as a function of simulation time.

the results obtained from the Kukol parameter set and the CHARMM36 or Berger parameter sets is also seen in the lipid aggregate topology which is further discussed below.

The mean aggregation numbers for the lipid aggregates in the last 50 ns of the three simulations are given in Table 7, and the average aggregation number is plotted as a function of simulation time in Figure 8b. From this plot it is seen that the eight micelles collapse into one large aggregate during the first 50 ns of simulation when modeled with the Kukol lipid force field. The final aggregate is depicted in Figure 9a. Similar clotting behavior is not observed in experiments and together with the underestimation of the free lipid concentration it emphasizes that the modifications made by Kukol to the GROMOS96 53A6 lipid parameters do not result in lipid parameters that are transferable to shorter tailed lipids, even though the strategy we have used to generate topology and parameters for DHPC is commonly used.[10,12,13] For both the CHARMM36 and Berger lipids the average aggregation number increases as compared to the CG simulation but levels off at around 40 lipids. In both simulations the initial micelles are stable and thus readily diffuse around in the simulation box. In many cases the headgroup regions of individual micelles are seen to overlap to such a degree that they are counted as one micelle even though they split apart again. The increase in aggregate size as compared to the CG simulation thus stems partly from micelles overlapping for a while and partly from smaller micelles actually fusing. As the lipid aggregates in the simulation box are interacting closely at numerous occasions during the simulation time, with ample possibility for fusion

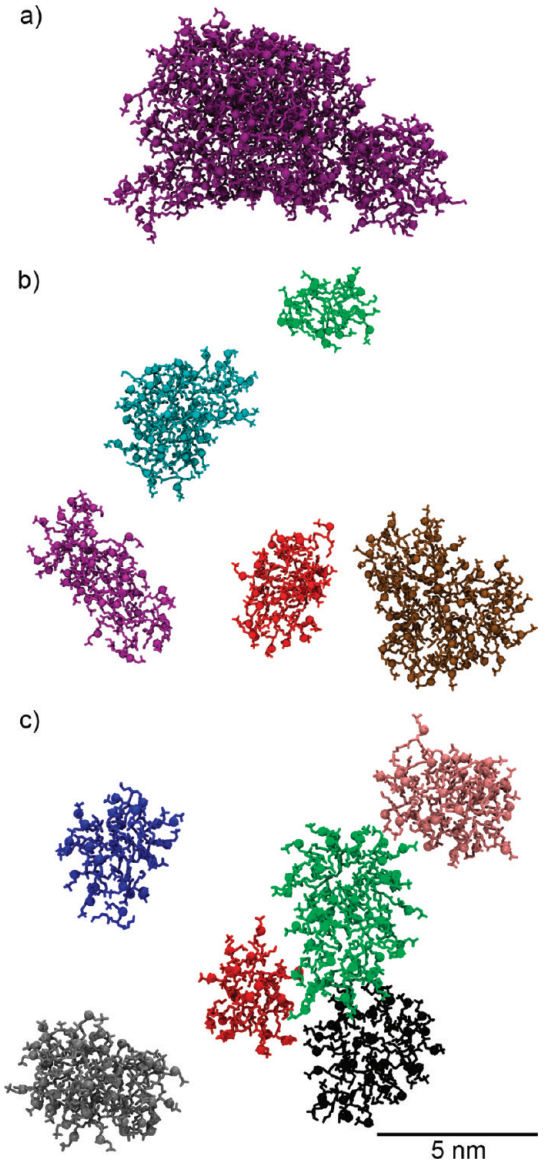

Figure 9. Lipid aggregates after 100 ns of atomistic simulations using **a**) the Kukol lipid parameters, **b**) the Berger lipid parameters, and **c**) the CHARMM36 lipid parameters.

without doing so, we do not expect that a longer simulation time would show a continued increase in average aggregation number. It is also seen from Figure 8b that the aggregation number has reached a steady level after ~50 ns of simulation. As the aggregation number of DHPC micelles has been found to be between 19 and 40 depending on the surrounding conditions (see Table 2), the aggregation numbers observed when using the CHARMM36 or Berger lipids are only slightly overestimating the aggregation. The short simulation time of 100 ns does not allow for the distribution of aggregation numbers to be fully equilibrated, but the observed aggregates seem to build up similar distributions when applying either the CHARMM36 or the Berger lipids (see Figure S4 in the Supporting Information) with an average around 40 lipids per micelle.

Overall the Berger and CHARMM36 lipid parameters reproduce a mixture of micelles where both the aggregation numbers and the free lipid concentration are close to experimental observations. The free lipid concentration seems

to be more realistically modeled with the atomistic force fields than with the CG model, but the aggregation numbers are slightly overestimated in the atomistic simulations. The Kukol lipid parameters fail in the description of DHPC in water, and care has to be taken when using these parameters outside the context of lipid bilayers as tested by Kukol.[13]

CONCLUSION

In this study a thorough investigation of the qualities and limitations of AA and CG MD modeling of DHPC lipid aggregates is presented. For the MARTINI CG force field[9] it is shown that the results are highly sensitive to the CG representation of both the lipid and the water. Contrary to previous studies of the influence of the chosen water model on lipid or surfactant aggregate structure,[26,48] we find that utilizing the polarizable water model[26] instead of the standard MARTINI water model[9] is essential for reproducing experimental observations. As the previous studies[26,48] only involved preassembled aggregates this could explain why a greater robustness toward the change in water model was observed. However, as a strong test against bias from the initial setup, simulations of lipid aggregates self-assembled in either standard or polarizable water and resolvated with the opposite water model were carried out. The results of this test are clear-cut; after a short time, the aggregates change to the same structure and topology as was observed for the simulations started with lipids at random positions in the same water model. The reason for the high sensitivity toward the representation of water observed for DHPC is instead to be found in the relative large hydrophilic component of this short-tailed lipid. It is also observed that the lipid aggregate size distributions are almost fully equilibrated within the 2 μs simulations, contrary to what has previously been reported for surfactants containing larger hydrophobic moieties than DHPC.[59,60]

For the preferred CG representation of DHPC in water the free lipid concentration is found to be slightly too low, but the distribution of aggregate sizes match with experimental observations, as the average aggregation number is found in the middle of the range of aggregation numbers determined experimentally.[14,16,21,44] For NaCl concentrations in the range 0−500 mM and temperatures in the range 285−325 K the model is found to reproduce experimental observations in a satisfactory manner, both qualitatively and quantitatively. Still, even though the CMC of DHPC should be practically temperature independent,[55] the free lipid concentration is found to increase with increasing temperature. This is a well-known defect arising from the crude representation of water interaction in CG representations,[47] and even the polarizable water model is not able to eradicate this flaw.

Following the CG simulations a selection of eight self-assembled CG micelles were selected for reverse coarse graining to an atomistic representation. This setup was then used for atomistic MD simulations using three different atomic resolution force fields: CHARMM36,[40] GROMOS96[31] with Berger lipid parameters,[32] and GROMOS96 with Kukol lipid parameters.[13] As standard procedure the topology and parameters for DHPC was based on the removal of methylene groups from longer tailed PC lipids.[10,12,13] This approach assumes transferability of the lipid parameters defined for e.g. DPPC to the more surfactant-like lipid DHPC. CHARMM and Berger lipids both successfully maintain stable micelles, which diffuse and exchange lipids within the 100 ns simulation time. The free lipid concentration is higher than observed in the CG simulation and thus more in line with experimental observations, and the aggregates are slightly larger being on the maximum of the experimentally observed range of aggregate sizes. However, the Kukol lipid parameters fail to describe DHPC in water as the initial micelles all fuse into one large aggregate during the first 50 ns. Also, the free lipid concentration is further lowered as compared to the already slightly too low concentrations observed for the CG simulations. The transferability usually assumed for lipid parameters is thus not valid for the Kukol parameters,[13] and great care should be taken if the lipids are used outside the context for which they have been parametrized.

From the results presented in this study, we conclude that using a DHPC MARTINI CG lipid with a single bead in each lipid tail solvated with the MARTINI polarizable water model can simulate micelles with properties in accordance with experimental data. Furthermore, the lipid aggregates can successfully be reverse coarse grained and modeled at atomic resolution using either the CHARMM36 parameter set or the Berger lipid parameters for GROMOS96. This way of modeling DHPC lipids will aid in future computational studies of micelles and other membrane mimics that contain DHPC.

ASSOCIATED CONTENT

Supporting Information

Data on aggregate size distributions. This material is available free of charge via the Internet at http://pubs.acs.org.

AUTHOR INFORMATION

Corresponding Author

*Phone: +45 8715 5567. Fax: +45 8715 4102. E-mail: lea@birc.au.dk or birgit@chem.au.dk.

Notes

The authors declare no competing financial interest.

ACKNOWLEDGMENTS

The authors thank Siewert-Jan Marrink for useful discussion on the use of the polarizable water model and the lipid model. Financial support is acknowledged from the Danish Research Foundation, the Danish Council for Independent Research | Natural Sciences, the Aarhus Graduate School of Science (AGSoS) as well as the Carlsberg, Lundbeck and Novo Nordisk Foundations. Computations were made possible through the Danish Centre for Scientific Computing in Aarhus.

REFERENCES

(1) Böckmann, R. A.; Caflisch, A. Spontaneous Formation of Detergent Micelles around the Outer Membrane Protein OmpX. *Biophys. J.* **2005**, *88*, 3191−3204.

(2) Pérez-Castells, J.; Martín-Santamaría, S.; Nieto, L.; Ramos, A.; Martínez, A.; de Pascual-Teresa, B.; Jiménez-Barbero, J. Structure of micelle-bound adrenomedullin, a first step towards the analysis of its interactions with receptors and small molecules. *Biopolymers* **2011**, *97*, 45−53.

(3) McKibbin, C.; Farmer, N. A.; Edwards, P. C.; Villa, C.; Booth, P. J. Urea Unfolding of Opsin in Phospholipid Bicelles? *Photochem. Photobiol.* **2009**, *85*, 494−500.

(4) Warschawski, D. E.; Arnold, A. A.; Beaugrand, M.; Gravel, A.; Chartrand, É.; Marcotte, I. Choosing membrane mimetics for NMR structural studies of transmembrane proteins. *Biochim. Biophys. Acta. Biomembr.* **2011**, *1808*, 1957−1974.

(5) Marrink, S. J.; Tieleman, D. P.; Mark, A. E. Molecular Dynamics Simulation of the Kinetics of Spontaneous Micelle Formation. *J. Phys. Chem. B* **2000**, *104*, 12165−12173.

(6) Sonntag, Y.; Musgaard, M.; Olesen, C.; Schiøtt, B.; Møller, J. V.; Nissen, P.; Thøgersen, L. Mutual adaptation of a membrane protein and its lipid bilayer during conformational changes. *Nat. Commun.* **2011**, *2*, 304.
(7) Dittmer, J.; Thøgersen, L.; Underhaug, J.; Bertelsen, K.; Vosegaard, T.; Pedersen, J. M.; Schiøtt, B.; Tajkhorshid, E.; Skrydstrup, T.; Nielsen, N. C. Incorporation of Antimicrobial Peptides into Membranes: A Combined Liquid-State NMR and Molecular Dynamics Study of Alamethicin in DMPC/DHPC Bicelles. *J. Phys. Chem. B* **2009**, *113*, 6928−6937.
(8) Mineev, K. S.; Bocharov, E. V.; Pustovalova, Y. E.; Bocharova, O. V.; Chupin, V. V.; Arseniev, A. S. Spatial Structure of the Transmembrane Domain Heterodimer of ErbB1 and ErbB2 Receptor Tyrosine Kinases. *J. Mol. Biol.* **2010**, *400*, 231−243.
(9) Marrink, S. J.; Risselada, H. J.; Yefimov, S.; Tieleman, D. P.; de Vries, A. H. The MARTINI Force Field: Coarse Grained Model for Biomolecular Simulations. *J. Phys. Chem. B* **2007**, *111*, 7812−7824.
(10) Jiang, Y.; Wang, H.; Kindt, J. T. Atomistic Simulations of Bicelle Mixtures. *Biophys. J.* **2010**, *98*, 2895−2903.
(11) Jiang, Y.; Kindt, J. T. Simulations of edge behavior in a mixed-lipid bilayer: Fluctuation analysis. *J. Chem. Phys.* **2007**, *126*, 045105−1−045105−9.
(12) Wang, H.; de Joannis, J.; Jiang, Y.; Gaulding, J. C.; Albrecht, B.; Yin, F.; Khanna, K.; Kindt, J. T. Bilayer Edge and Curvature Effects on Partitioning of Lipids by Tail Length: Atomistic Simulations. *Biophys. J.* **2008**, *95*, 2647−2657.
(13) Kukol, A. Lipid Models for United-Atom Molecular Dynamics Simulations of Proteins. *J. Chem. Theory Comput.* **2009**, *5*, 615−626.
(14) Chou, J. J.; Baber, J. L.; Bax, A. Characterization of phospholipid mixed micelles by translational diffusion. *J. Biomol. NMR* **2004**, *29*, 299−308.
(15) Burns, R. A.; Roberts, M. F.; Dluhy, R.; Mendelsohn, R. Monomer-to-micelle transition of dihexanoylphosphatidylcholine: carbon-13 NMR and Raman studies. *J. Am. Chem. Soc.* **1982**, *104*, 430−438.
(16) Tausk, R. J. M.; Esch, J. v.; Karmiggelt, J.; Voordouw, G.; Overbeek, J. T. G. Physical chemical studies of short-chain lecithin homologues. II Micellar weights of dihexanoyl- and diheptanoyllecithin. *Biophys. Chem.* **1974**, *1*, 184−203.
(17) Tausk, R. J. M.; Oudshoorn, C.; Overbeek, J. T. G. Physical chemical studies of short-chain lecithin homologues III. Phase separation and light scattering studies on aqueous dioctanoyllecithin solutions. *Biophys. Chem.* **1974**, *2*, 53−63.
(18) Helmut, H. Short-chain phospholipids as detergents. *Biochim. Biophys. Acta. Biomembr.* **2000**, *1508*, 164−181.
(19) De Haas, G. H.; Bonsen, P. P. M; Pieterson, W. A.; Van Deenen, L. L. M. Studies on Phospholipase A and its Zymogen from Porcine Pancreas: III. Action of the Enzyme on Short-chain Lecithins. *Biochim. Biophys. Acta* **1971**, *239*, 252−266.
(20) Johnson, R. E.; Wells, M. A.; Rupley, J. A. Thermodynamics of dihexanoylphosphatidylcholine aggregation. *Biochemistry (N. Y.)* **1981**, *20*, 4239−4242.
(21) Lin, T. L.; Chen, S. H.; Gabriel, N. E.; Roberts, M. F. The use of small-angle neutron scattering to determine the structure and interaction of dihexanoylphosphatidylcholine micelles. *J. Am. Chem. Soc.* **1986**, *108*, 3499−3507.
(22) Hauser, H. Polar group conformation of phosphatidylcholine. Effect of solvent and aggregation. *Biochemistry* **1980**, *19*, 366−373.
(23) Roholt, O. A.; Schlamowitz, M. Studies of the use of dihexanoyllecithin and other lecithins as substrates for phospholipase A: With addendum on aspects of micelle properties of dihexanoyllecithin. *Arch. Biochem. Biophys.* **1961**, *94*, 364−379.
(24) Hess, B.; Kutzner, C.; van, d. S.; Lindahl, E. GROMACS 4: Algorithms for Highly Efficient, Load-Balanced, and Scalable Molecular Simulation. *J. Chem. Theory Comput.* **2008**, *4*, 435−447.
(25) Monticelli, L.; Kandasamy, S. K.; Periole, X.; Larson, R. G.; Tieleman, D. P.; Marrink, S. The MARTINI Coarse-Grained Force Field: Extension to Proteins. *J. Chem. Theory Comput.* **2008**, *4*, 819−834.
(26) Yesylevskyy, S. O.; Schäfer, L. V.; Sengupta, D.; Marrink, S. J. Polarizable Water Model for the Coarse-Grained MARTINI Force Field. *PLoS Comput. Biol.* **2010**, *6*, e1000810−1-e1000810−16.
(27) Marrink, S. J.; de Vries, A. H.; Mark, A. E. Coarse Grained Model for Semiquantitative Lipid Simulations. *J. Phys. Chem. B* **2004**, *108*, 750−760.
(28) Copestake, A. P.; Neilson, G. W.; Enderby, J. E. The structure of a highly concentrated aqueous solution of lithium chloride. *J. Phys. C* **1985**, *18*, 4211−4216.
(29) Berendsen, H. J. C.; Postma, J. P.; van Gunsteren, W. F.; DiNola, A.; Haak, J. R. Molecular dynamics with coupling to an external bath. *J. Chem. Phys.* **1984**, *81*, 3684−3690.
(30) Rzepiela, A. J.; Sengupta, D.; Goga, N.; Marrink, S. J. Membrane poration by antimicrobial peptides combining atomistic and coarse-grained descriptions. *Faraday Discuss.* **2010**, *144*, 431−443.
(31) Oostenbrink, C.; Villa, A.; Mark, A. E.; Van Gunsteren, W. F. A biomolecular force field based on the free enthalpy of hydration and solvation: The GROMOS force-field parameter sets 53A5 and 53A6. *J. Comput. Chem.* **2004**, *25*, 1656−1676.
(32) Berger, O.; Edholm, O.; Jähnig, F. Molecular dynamics simulations of a fluid bilayer of dipalmitoylphosphatidylcholine at full hydration, constant pressure, and constant temperature. *Biophys. J.* **1997**, *72*, 2002−2013.
(33) Essmann, U.; Perera, L.; Berkowitz, M. L.; Darden, T.; Lee, H.; Pedersen, L. G. A smooth particle mesh Ewald method. *J. Chem. Phys.* **1995**, *103*, 8577−8593.
(34) Berendsen, H. J. C.; Postma, J. P.; van Gunsteren, W. F.; Hermans, J. Interaction Models for Water in Relation to Protein Hydration. In *Intermolecular Forces*; Pullman, B., Ed.; D. Reidel Publishing: 1981; pp 331−342.
(35) Hess, B.; Bekker, H.; Berendsen, H. J. C.; Fraaije, J. G. E. M. LINCKS: A Linear Constraint Solver for Molecular Simulations. *J. Comput. Chem.* **1997**, *18*, 1463−1472.
(36) Hess, B. P-LINCS: A Parallel Linear Constraint Solver for Molecular Simulation. *J. Chem. Theory Comput.* **2008**, *4*, 116−122.
(37) Humphrey, W.; Dalke, A.; Schulten, K. VMD: Visual Molecular Dynamics. *J. Mol. Graphics* **1996**, *14*, 33−38.
(38) Shih, A. Y.; Arkhipov, A.; Freddolino, P. L.; Schulten, K. Coarse Grained Protein -Lipid Model with Application to Lipoprotein Particles. *J. Phys. Chem. B* **2006**, *110*, 3674−3684.
(39) Shih, A. Y.; Freddolino, P. L.; Arkhipov, A.; Schulten, K. Assembly of lipoprotein particles revealed by coarse-grained molecular dynamics simulations. *J. Struct. Biol.* **2007**, *157*, 579−592.
(40) Klauda, J. B.; Venable, R. M.; Freites, J. A.; O'Connor, J. W.; Tobias, D. J.; Mondragon-Ramirez, C.; Vorobyov, I.; MacKerell, A. D.; Pastor, R. W. Update of the CHARMM All-Atom Additive Force Field for Lipids: Validation on Six Lipid Types. *J. Phys. Chem. B* **2010**, *114*, 7830−7843.
(41) Phillips, J. C.; Braun, R.; Wang, W.; Gumbart, J.; Tajkhorshid, E.; Villa, E.; Chipot, C.; Skeel, R. D.; Kalé, L.; Schulten, K. Scalable Molecular Dynamics with NAMD. *J. Comput. Chem.* **2005**, *26*, 1781−1802.
(42) Jorgensen, W. L.; Chandrasekhar, J.; Madura, J. D.; Impey, R. W.; Klein, M. L. Comparison of simple potential functions for simulating liquid water. *J. Chem. Phys.* **1983**, *79*, 926−935.
(43) Feller, S. E.; Zhang, Y.; Pastor, R. W.; Brooks, B. R. Constant pressure molecular dynamics simulation: The Langevin piston method. *J. Chem. Phys.* **1995**, *103*, 4613−4621.
(44) Lipfert, J.; Columbus, L.; Chu, V. B.; Lesley, S. A.; Doniach, S. Size and shape of detergent micelles determined by small-angle X-ray scattering. *J. Phys. Chem. B* **2007**, *111*, 12427−12438.
(45) Baoukina, S.; Monticelli, L.; Amrein, M.; Tieleman, D. P. The Molecular Mechanism of Monolayer-Bilayer Transformations of Lung Surfactant from Molecular Dynamics Simulations. *Biophys. J.* **2007**, *93*, 3775−3782.
(46) Marrink, S. J.; Lindahl, E.; Edholm, O.; Mark, A. E. Simulation of the Spontaneous Aggregation of Phospholipids into Bilayers. *J. Am. Chem. Soc.* **2001**, *123*, 8638−8639.

(47) Sanders, S. A.; Panagiotopoulos, A. Z. Micellization behavior of coarse grained surfactant models. *J. Chem. Phys.* **2010**, *132*, 114902−1−114902−9.
(48) Sangwai, A. V.; Sureshkumar, R. Coarse-Grained Molecular Dynamics Simulations of the Sphere to Rod Transition in Surfactant Micelles. *Langmuir* **2011**, *27*, 6628−6638.
(49) Hayter, J. B.; Penfold, J. Determination of micelle structure and charge by neutron small-angle scattering. *Colloid Polym. Sci.* **1983**, *261*, 1022−1030.
(50) Imae, T.; Ikeda, S. Characteristics of rodlike micelles of cetyltrimethylammonium chloride in aqueous NaCl solutions: Their flexibility and the scaling laws in dilute and semidilute regimes. *Colloid Polym. Sci.* **1987**, *265*, 1090−1098.
(51) Ikeda, S. Stability of spherical and rod-like micelles of ionic surfactants, in relation to their counterion binding and modes of hydration. *Colloid Polym. Sci.* **1991**, *269*, 49−61.
(52) Magid, L. J.; Han, Z.; Warr, G. G.; Cassidy, M. A.; Butler, P. D.; Hamilton, W. A. Effect of Counterion Competition on Micellar Growth Horizons for Cetyltrimethylammonium Micellar Surfaces: Electrostatics and Specific Binding. *J. Phys. Chem. B* **1997**, *101*, 7919−7927.
(53) Tausk, R. J. M.; Karmiggelt, J.; Oudshoorn, C.; Overbeek, J. T. G. Physical chemical studies of short-chain lecithin homologues. I. Influence of the chain length of the fatty acid ester and of electrolytes on the critical micelle concentration. *Biophys. Chem.* **1974**, *1*, 175−183.
(54) Tausk, R. J. M.; Overbeek, J. T. G. Physical chemical studies of short-chain lecithin homologues IV. A simple model for the influence of salt and the alkyl chain length on the micellar size. *Biophys. Chem.* **1974**, *2*, 175−179.
(55) van Dam, L.; Karlsson, G.; Edwards, K. Direct observation and characterization of DMPC/DHPC aggregates under conditions relevant for biological solution NMR. *Biochim. Biophys. Acta, Biomembr.* **2004**, *1664*, 241−256.
(56) Malliaris, A.; Le Moigne, J.; Sturm, J.; Zana, R. Temperature dependence of the micelle aggregation number and rate of intramicellar excimer formation in aqueous surfactant solutions. *J. Phys. Chem.* **1985**, *89*, 2709−2713.
(57) Israelachvili, J. N.; Mitchell, D. J.; Ninham, B. W. Theory of self-assembly of hydrocarbon amphiphiles into micelles and bilayers. *J. Chem. Soc., Faraday Trans. 2* **1976**, *72*, 1525−1568.
(58) Jorgensen, W. L.; Tirado-Rives, J. The OPLS potential functions for proteins - energyminimizations for crystals of cyclic-peptides and crambin. *J. Am. Chem. Soc.* **1988**, *110*, 1666−1671.
(59) Velinova, M.; Sengupta, D.; Tadjer, A. V.; Marrink, S. Sphere-to-Rod Transitions of Nonionic Surfactant Micelles in Aqueous Solution Modeled by Molecular Dynamics Simulations. *Langmuir* **2011**, *27*, 14071−14077.
(60) Levine, B. G.; LeBard, D. N.; DeVane, R.; Shinoda, W.; Kohlmeyer, A.; Klein, M. L. Micellization Studied by GPU-Accelerated Coarse-Grained Molecular Dynamics. *J. Chem. Theory Comput.* **2011**, *7*, 4135−4145.